T.C

ALTINBAŞ UNIVERSITY

Graduate School of Science and Engineering

Electrical and Computer Engineering

ENERGY HARVESTING FROM RF SIGNALS AND ULTRA-HIGH VOLTAGE TRANSMISSION LINES (UHVTL) FOR WIRELESS CHARGING OF UAV

MAIGALISA YOHANNA

Master's Thesis

Thesis Supervisor:
Dr. Çağatay AYDIN

Istanbul, 2020

ENERGY HARVESTING FROM RF SIGNALS AND ULTRA-HIGH VOLTAGE TRANSMISSION LINES (UHVTL) FOR WIRELESS CHARGING OF UAV

by

Maigalisa Yohanna

Department of Electrical and Computer Engineering

Submitted to the Graduate School of Science and Engineering

in partial fulfillment of the requirements for the degree of

Master of Science

ALTINBAŞ UNIVERSITY

2020

This is to certify that we have read this thesis and that in our opinion it is fully adequate, in scope and quality, as a thesis for the degree of Master of Science

Asst. Prof. Çağdaş Doğu ATILLA

Co-Supervisor

Asst. Prof. Çağatay AYDIN

Supervisor

Examining Committee Members (first name belongs to the chairperson of the jury and the second name belongs to supervisor)

Asst. Prof. Muhammad ILYAS	School of Engineering and Natural Sciences, Altınbaş University	
Asst. Prof. Çağatay AYDIN	School of Engineering and Natural Sciences, Altınbaş University	
Asst. Prof. Cahit KARAKUŞ	Engineering and Architecture, Esenyurt Unıversıty	

I certify that this thesis satisfies all the requirements as a thesis for the degree of Master of Science.

Asst. Prof. Çağatay AYDIN

Head of Department

Prof. Oğuz BAYAT

Director

Approval Date of Graduate School of Science and Engineering: ____/____/____

I hereby declare that all information in this document has been obtained and presented in accordance with academic rules and ethical conduct. I also declare that, as required by these rules and conduct, I have fully cited and referenced all material and results that are not original to this work.

Maigalisa Yohanna

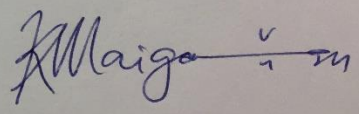

DEDICATION

I dedicate this work to God Almighty for keeping me alive and healthy to get through it, to my beautiful wife Danielle Villasana for being a sponsor and moral support, without whom this project wouldn't have been possible, and to my lovely family for their encouragement and care.

ACKNOWLEDGEMENTS

I would love to acknowledge my supervisor and co-supervisor for guiding and providing me with resources, materials, and references throughout my research, without which this work would not be possible. Furthermore, I acknowledge the immense contribution of Prof. Cahit Karakuş for his supervision and guidance through my research on energy harvesting theories and concepts. Also, Durrie Bouscaren, for meticulously reviewing and editing this thesis script, and last but not least, the QuickField team that helped run my simulations on a professional version of their software, free of charge.

ABSTRACT

ENERGY HARVESTING FROM RF SIGNALS AND ULTRA-HIGH VOLTAGE TRANSMISSION LINES (UHVTL) FOR WIRELESS CHARGING OF UAV

Yohanna, Maigalisa,

M.S, Graduate School of Science and Engineering, Altınbaş University,

Supervisor: Dr. Çağatay Aydin

Co-Supervisor: Dr. Çağdaş Atilla

Date: February 2020

Pages: 62

UAVs are becoming increasing reliable in mission-critical assignments and surveillance. Therefore, it is essential to find methods to keep them charged and functioning at all times, without interruption. It's for this purpose that we came up with a charging solution for the UAV, which will enable it charge wirelessly using RF signals or while hovering around any Ultra-High Voltage Transmission Line (UHVTL). Research has already been done in energy harvesting and WPT for small powered devices within close proximity to RF sources and high voltage power lines. In one case, experiments were conducted using solenoid coil [1]. In another, more effective case, researchers used a modified Bow-tie shaped solenoid coil[2]. However, both cases suffered from a limited proximity to the harvesting source – the power lines. This made the authors to compromise between size and weight to achieve desired power. This design is built to be integrated into a UAV for fast charging during mission critical or surveillance tasks. This means that the UAV will hover in close proximity to the transmission power line, thereby increasing the magnetic field that cuts through the harvesting coil/core. This increases the overall power harvested. The

UAV will also carry antennas that will couple with RF waves when it is introduced to the field to generate power. The RF component will host an array of high gain directional antennas of different receiver frequencies. The harvesting coil design is a modified version of the Bow-tie model core [2] and also a size reduction – from a proposed $40cm$ length to $15cm$. It weighs a little over $1.5kg$, while still achieving a strong Magnetic flux, in the region of approximately $1T$. The placement of the coil will be closer to the transmission line, in range of about $60\mu T$ magnetic flux density to induce about $0.5mA$ of current. This is achieved at a distance of less than $5m$ from the top phase lines, as opposed to the $5m$ above ground level measurement $11\mu T$ used in the reference research [2].

Keywords: Electromagnetic Induction, Energy Harvesting, Wireless Power Transfer, UAV, Ultra-High Voltage Transmission Lines, RF Energy Harvesting

TABLE OF CONTENTS

Pages

LIST OF TABLES ..... **xi**

LIST OF FIGURES ..... **xii**

LIST OF ABBREVIATIONS ..... **xiv**

1. INTRODUCTION **15**

1.1 MOTIVATION 15

2. WIRELESS POWER TRANSFER THEORIES **17**

2.1 LITERATURE REVIEW 17

2.2 THEORY OF ENERGY SOURCES 20

2.2.1 Base Transceiver Station (BTS) 20

2.2.2 Ultra-High Voltage Transmission Power Lines (UHVTL) 21

2.3 CONCLUSION 22

3. SYSTEM MODEL **23**

3.1 SYSTEM DESCRIPTION 23

3.1.1 Radiative Far/Near Field Reception 23

3.1.1.1 Antenna array 23

3.1.1.2 Rectenna 23

3.1.1.3 Regulator 24

3.1.2 Inductive Power Reception 25

3.1.2.1 The Coil 26

3.2 FORMULATION 28

3.2.1 Wireless Energy Harvesting from BTS 28

3.2.2 Energy Harvesting from High Voltage Transmission Lines 33

4. ANALYSIS AND RESULTS **41**

4.1 RF ENERGY HARVESTING 41

4.2 UHVTL ENERGY HARVESTING 43

4.2.1 Coil Model 51
5. CONCLUSION 55
5.1 CONCLUSION 55
5.2 FUTURE WORK 56
REFERENCES 57
APPENDIX A……...62

LIST OF TABLES

Pages

Table 2.1: Comparing different frequency bands for RF WPT (adopted from [10]) 21

Table 4.1: Simulation parameter for RF energy harvest..... 41

Table 4.2: Result showing received power at different distance ranges for two separate considered frequency bands 42

Table 4.3: Estimated power harvested from a given scenario 43

LIST OF FIGURES

Pages

Figure 3.1: Schematic Showing the Rectenna circuit consisting of an N-Stage Cockcroft-Walton Charge Pump (Voltage Multiplier) 24

Figure 3.2: Diagram showing the RF harvesting blocks from the multiple frequency, different direction reception antennas, to the charging phase 25

Figure 3.3: Magnetic Field generated around a UHVTL that induces current in a parallel coil .. 27

Figure 3.4: A Flow diagram showing a detailed layout of the system, from input induction source to UAV battery unit. 28

Figure 3.5: Magnetic Force field between two current carrying conductors 33

Figure 3.6: Presence of capacitive coupling acting on transmission lines..... 36

Figure 3.7: Cross-sectional view of parallel conductors showing their relationship with respect to their distance. The Current direction is into the paper. 37

Figure 3.8: An inductive Circuit 39

Figure 4.1: Plot of received power vs distance between transmitting and receiving antenna 41

Figure 4.2: Dimension of the simulated UHVTL tower showing the 3 x 2 transmission cables hanging from their insulators. 44

Figure 4.3: AC conduction simulation results showing the six transmission cables and the effective electric fields strength formed around them (simulation was performed using actual scale)..... 45

Figure 4.4: AC Conduction simulation showing resultant floating voltage around transmission lines 45

Figure 4.5: AC Magnetic analysis showing the magnetic flux density around transmission lines 46

Figure 4.6: AC Magnetic analysis showing an instance capture of the magnetic field's potential radiation around the transmission lines..... 46

Figure 4.7: AC Conduction plot of electric field strength from cross-section taken: (Top) at the symmetrical center, and (Bottom) 10 meters away from the center of transmission tower 48

Figure 4.8: Floating voltage around the transmission line plot taken from the: (Top) symmetrical center, and (Bottom) 10 meters from center of the tower's reference point..... 49

Figure 4.9: Magnetic flux density around transmission line plot taken from the: (Top) symmetrical center, and (Bottom) 10 meters from center of the tower's reference point..... 50

Figure 4.10: Yuan et al. Bow-tie Coil (Top), our first modification to the Bow-tie Coil model (center), Curved Core Design (bottom) 51

Figure 4.11: Bow-Tie model proposed by Yuan et al. [2] with uniform internal magnetic flux density of approximately 0.25T in the core 52

Figure 4.12: First attempt on Bow-Tie modification showing an average uniform magnetic flux density of 0.25T just like the original model. 53

Figure 4.13: Final modification we call the Mushroom Head Core. This is the result of uniform magnetic flux density, which is almost 1T. 53

LIST OF ABBREVIATIONS

UAV	Unmanned Aerial Vehicle
UHVTL	Ultra-High Voltage Transmission Line
RF	Radio Frequency
WPT / WPH	Wireless Power Transfer / Wireless Power Harvesting
BTS	Base Transceiver Station

1. INTRODUCTION

Drones, or Unmanned Aerial Vehicles (UAVs), are increasingly important in everyday life. They are used in many disciplines and professions because they can be programmed or designed to perform different tasks with increasing degrees of accuracy. Their ability to fly, give aerial assessments / results, and their ease of reaching target locations with little or no obstacles in good time makes them better choices for a variety of tasks. They are deployed in emergency situations, surveillance, geo mapping, goods delivery, photography, cinematography, etc. UAVs come in different sizes, functions, and capacities. They can easily be modified for their functions. UAVs are designed to cargo or functional equipment, such as cameras, test equipment, goods or medical kits. The machine's structural components – batteries, frames, motors, etc. – these weights impact the overall flight time of UAVs. One of the major criteria for checking the performance of UAVs is flight time – the time it takes a UAV to fly before it requires charging. Energy or power required to complete a necessary flight time is the key consideration to every successful or bestselling UAV. It is of utmost importance to narrow the field of UAV's down to utility or essential aircraft (such as those used in emergency and rescue operations or those used for 24-hour security surveillance), their runtime and availability is of topmost importance in mission critical application and overall performance efficiency, as it is the focus of this thesis.

1.1 MOTIVATION

As it is stated in the law of Thermodynamics: energy can neither be created nor destroyed, but it can be transformed from one form to another [3]. This definition makes every matter existing on our planet a potential energy source. There are several sources of energies that are currently exploited on a global scale to improve efficiency, and provide more flexible access. It's important to maximize the use of abundant natural resources through conversion methods and a variety of power options to conserve these energies for the increasing demands arising from portable devices. Some forms of energy conversion are inspired by the technological tilt towards mobile and portable electronic equipment relying on battery power. As a battery discharges while a user is on the move, the device's battery capacity becomes the limiting factor while performing a task. Lots of thought has been put to addressing the challenges that come with mobility and portability, prompting engineers to develop energy saving and management systems to improve the run time

of devices. In some cases, trade-offs are made. This limits the designed performance of many devices. But no matter how much work is put into the longevity of a battery's life, charging will always be required. To address this, attention was focused on fast, accessible and easy charging. This inspired the development of wireless power transfer (WPT).

Wireless power transfer (WPT) is a solution to mobile and convenient charging. This is a technology by which devices are charged or powered through electromagnetic means, without using a physical connecting wire. This principle was first studied and patented by Tesla over a century ago [4]. Now it has become more relevant and worthy of research. WPT electricity transfer is done by using electromagnetic waves in the form of low frequency current induction (magnetic field in close proximity), radiation as in high frequency Radio Frequency (RF) or Microwave emission through a given effective distance [5].

Many wireless devices communicate using RF or Microwave signals as carriers. These carriers make the air space they occupy ready for the frequency of a user's communications signal to flow through it. In other words, these transmission frequencies are potential energy resources laying idle around devices that could be used for charging.

This thesis will discuss harvesting energies – of significant values – from RF frequencies being transmitted in the air medium and electromagnetic field around Ultra-High Voltage Transmission Lines (UHVTL).

2. WIRELESS POWER TRANSFER THEORIES

This chapter will review some of the research completed by other scholars in WPT, which will lay a foundation for this work and a theory of the energy sources.

2.1 LITERATURE REVIEW

The research in the fields of WTP and induction coupling will be discussed, and particular references made to the key components relating to the scope of this thesis.

The evolution of wireless access networks to increase data capacity is taking over the airwaves now. Unlike earlier techniques of wireless communication, higher frequencies at a lower transmission power are employed to achieve higher data rates. In a paper by Bhushan et al. [6] on network densification for 5G access, the authors propose how a complete network architecture can be disintegrated into smaller heterogeneous networks or neighborhood cells – small cell technology, as described in [7]. This achieves higher throughput and access among increasing user populations. The authors also discuss the concept of Device-to-Device communications, and how battery intensive this solution can be. It may be assumed that with all of these solutions, there will be abundant frequencies. However, this is not the case. With low transmission power, there will be insignificant harvested power. Considering a subscriber's usage pattern, it is noted that all heavy traffic (data channels) will shift from the long range, low frequency, high transmission power channels to short range, high frequency, and low power transmission channels. This leaves the available, idle RF energy in the suitable channel for harvesting.

A typical harvesting model is introduced by Tran et al. [8]. It is deployed to harvest energy from transmitted RF power. They consider the effect different forms of antennas and rectification components must have on the overall received output of the harvested power. The model they present uses high gain antennas to receive transmitted frequencies, then passed through an impedance matching circuit, which rectifies the signal. It is then passed through a management system before dispensing to the device. However, their work is limited to an almost ideal environment scenario. When the conditions become unstable – in terms of losses and miniaturization – it may encounter some setbacks. Also, as it is common with Wireless Power

Harvesting (WPH), there is only a certain amount of significant energy that can be harvested. This is without taking into account the transmission power of the frequency to be harvested and proximity to the transmission source, which can greatly affect the received power output [9]. Furthermore, one must consider the roles that antennas and frequencies play on possible power outputs at a given distance from the transmitting source. A publication by Galinina et al. [10] proposes a model of charging wearable devices in a densified network. They observe that, there could be charging interruptions as users roam about or beyond coverage areas, but they lament that more WPH efficient spectrum bands are inaccessible.

It should also be noted that the frequencies used in WPT are not ionizing. This means they lay in the non-ionizing range of the electromagnetic spectrum, and makes them harmless to human exposure. Even in the medical field, the application of WPT for charging implants is widely researched [11],[12]. Ultra-High Frequencies that are non-ionizing can pose threats to human cells when a direct contact is maintained at close proximity over a long period of time [13]. Effects of prolonged exposure could be minimized or prevented, as discussed by Moradi et al. [14]. This by no means poses a health effect or mutation to the resident population.

It is important to note that some research has been made in frequency resonance coupling. In frequency coupling systems of WPT, two coils are placed apart and at a set resonance frequency. Through coupling, power is transferred [12]. This method is used in many close contact device charging systems, because such coupling can only be effective when the distance of separation between the coils is small. Research like [15] and [16] have worked to increase this effective distance of separation, and succeeded in the gain of a few centimeters. Another approach to frequency resonance coupling [17], [18] is shown in the work by Paul and Sarma [19], where two inductive coils are placed at a significant distance apart. They are both set to work on different resonance frequencies, using a method known as the adiabatic and transitionless quantum driving (TQD) algorithm to transfer power. At the end of their analysis they reached the conclusion that the TQD outperformed the adiabatic in terms of coupling time, which caused a delay in the adiabatic and an overall decrease in efficiency.

Based on the reviewed research, in order to harvest significant power wirelessly, at least one of these three conditions must be applied: high transmission power, closer proximity to the transmission source, or a high gain directional receiver antenna (or coils in the case of resonance).

Also, because WPT is not only used to avoid the necessity of connection interfaces and port access, other considerations can take priority, such as placing the charging unit away from the device to be charged, to allow room for some degree of roaming freedom away from the source during charging.

Conversely, an electric field induction system works with the magnetic field generated around an AC conductor, as demonstrated by Lu et al. in [17]. This is the case in alternating current technologies as well, because of the 'charging current' effect. This is essentially the charging and discharging states produced by AC through a 50Hz or 60Hz cycle. This cycle is similar to the principle a generator or alternator uses to produce electricity, obeying Faraday and Lenz's Laws [20]. The proximity of a harvesting unit to the conducting wires plays a big role in achieving higher efficiency, as well as in cases where clamp meters are used. A reference to this principle appears in Caxias et al.[21], related to the design of a robot for the inspection of transmission lines. Energy harvesting devices are placed closer to the conducting source because the field strength is strongest near the conductor. White et al.[22], in their research on energy harvesting from a power line, demonstrate the use of an electric field guide around a conducting wire. This is then used to channel the field strength around the wire towards an induction coil placed inside the guide. It was brilliant work, but considering the fact that power lines are out of reach, placing a blanket of field guides around such cables is practically impossible. Their solution may be limited to a certain level of power distribution line. A proposed research with similar proximity limitation was also made in the experiment by Gupta et al. [23]. However, when there is an obvious impediment to having practically close access to the proposed charging source, there must be other ways to harvest energy from such Ultra-High Voltage Transmission Lines (UHVTL).

To get further insight into electric field induction in transmission lines, consider a publication by Horton et al. [24] on induced voltage in parallel transmission lines. The authors propose a formula – in an effort to de-energize transmission lines – for calculating the voltage induced in a conductor laying parallel to another voltage carrying a conductor. Their proposed method considers the distance of separation and capacitive properties between both lines, as well as between the individual transmission lines and the ground. They obtain results in a few thousand volts at about 500m. A current flow from a center distance of about 50 feet from a 161kV line. This is quite substantial. In a separate analysis conducted by Luo et al. [25] on an UHVTL, they

use a three phase UHVTL. They base their analysis of the induced voltage on three variables, namely; resultant height, whether it is ground and ungrounded, and the parallel length of the transmission lines. The results are also significant. The results from these two analysis affirms that electric field strength reduces with distance [26]; but at higher power level, the electric field will also be larger, increasing the effective field strength radius. Therefore, at an Ultra-High voltage energy level, we can harvest power from a reasonable distance from the power line.

2.2 THEORY OF ENERGY SOURCES

In order to harvest energy wirelessly, electromagnetic energy sources are required. In this thesis we will consider two electromagnetic sources for energy harvesting: Base Transceiver Stations (BTS) and Ultra-High Voltage Transmission Lines (UHVTL). These transfers use different theories. Energy harvesting from BTS requires the use of radiated frequency at a significant power level and high efficiency (Gain) directional receiver antennas; whereas energy harvesting from UHVTL requires induction coils.

2.2.1 Base Transceiver Station (BTS)

BTS are designed to send information signals or packets through airwaves using what is known as carrier frequencies, which are electromagnetic in nature. The suitable electromagnetic frequencies needed for wireless power harvesting generally fall in the category of the frequency spectrum known as Radio Frequency (RF). Frequency radiation through RF can be classified in two forms; Far Field (Fraunhofer region) radiation and Near Field (Fresnel region) radiation. While discussing these two forms of RF propagations, we will consider factors such as the type of frequency transmitted, transmission antenna (antenna gain and orientation), transmission power and the effective radius of charge.

In terms of transmission frequencies, low frequencies are known to travel very far distances due to their long wavelengths. However, to transmit at such frequencies, an antenna length or diameter must match the wavelength. This allows low frequencies to be transmitted through a more realistic Half Wavelength or Quarter Wavelength antenna [27]. Such low frequency transmissions are sometimes referred to as Ground Transmission because the earth's surface helps propagate the transmitted frequency over very far distances, assuming no obstructions along the earth's curvature

or relief. The low frequencies are far down in the category of energy levels and ionization. This brings us to the idea of high frequency transmission. High frequencies have short wavelengths and low penetration power. Because they have short wavelengths, the size of their transmission antennas are considerably small, making it possible to transmit at full wavelength. However, unlike the low frequencies, ground transmission is not needed here. Its propagation distance is also limited. High Frequencies transmit at higher energy levels, thereby making them suitable for Near Field transmission. Table 1 shows a comparison of different frequencies and their possible RF charging energies. It can be deduced that the harvesting of energy at near field will generate more power.

Table 2.1: Comparing different frequency bands for RF WPT (adopted from [10])

Parameter[1]	ISM (industrial, scientific, and medical) bands						Cellular bands									
Band	915 MHz		2.4 GHz		5.8 GHz		850 MHz		1.7 GHz		2.1 GHz		1.9 GHz		2.5 GHz	
Wavelength, m	0.33		0.12		0.05		0.35		0.18		0.14		0.16		0.12	
Array size[2], m	0.33x0.33		0.12x0.12		0.05x0.05		0.35x0.35		0.18x0.18		0.14x0.14		0.16x0.16		0.12x0.12	
	Omni	Direct.	Omni	Direct.	Omni	Direct.	Omni	Direct.	Omni	Direct.	Omni	Direct.	Omni	Direct.	Omni	Direct.
Energy radius, m	10.57	34.85	3.95	13.01	1.67	5.50	11.38	37.51	5.69	18,76	4.60	15.18	5.09	16.78	3.87	12.75
$P_{harvested}$[3], μW	11.17	121.44	1.56	16.94	0.28	3.02	12.94	140.73	3.24	35.18	2.12	23.06	2.59	28.16	1.50	16.27
Replenishment rate[4], %	123	2329	-69	242	-94	-40	159	2715	-35	604	-58	361	-48	463	-70	225
Energy positive range[5], m	14.95	49.28	5.58	18.41	2.36	7.77	16.09	53.05	8.04	26.53	6.51	21.47	7.20	23.73	5.47	18.04
Support time[6], min	8.11	0.43	N/A[7]	4.19	N/A	N/A	6.30	0.37	N/A	1.66	N/A	2.77	N/A	2.16	N/A	4.44

[1] Parameters used for estimation are: transmitter antenna gain (omni-directional/directional) 2.15/14.51dBi, receiver gain 0dBi, WET efficiency 50%, sensitivity = -20dB, consumed power (discharge rate) 5μW, radiated power 1/0.63W (omni-directional/directional)
[2] Assuming 3x3 square transmitter array with $1/2$ wavelength separation
[3] Harvested power at reference distance 10m
[4] Energy replenishment rate at 10m = (harvested power/consumed power -1)·100%
[5] Maximum distance where harvested power≥consumed power
[6] Time of harvesting to support $N = 10$ min of autonomous work at 10m
[7] Not available due to feasibility constraints

2.2.2 Ultra-High Voltage Transmission Power Lines (UHVTL)

High voltage power lines radiate high frequencies during transmission, but the UHVTL line, like any other form of electricity distribution source, radiates only 50Hz or 60Hz (depending on a region or country's standard). This is the standard frequency for every power generation plant. If such frequency is to be used for WPT through radiation, it will require an impractically long antenna in the form of $3 \times 10^8/50 = 6{,}000\ km$ to transmit power, which is not feasible. This bring us to the induction theory as a method to harvest such energies from power lines. Just like the operation of transformers, the proposed model will harvest energy using an induction coil that is separated by some distance from the UHVTL. This induction happens when the magnetic field created around the Ultra-High Voltage cables is radiated through the surrounding air medium, and

an induction coil is introduced into the generated field to cause current to flow through winding coil conductors.

2.3 CONCLUSION

Most of the proposed energy harvesting systems that are reviewed in this chapter are in some ways targeting specific low power applications. One thing that WPT technologies all have in common is the fact that the harvested power is not sufficient for large scale device charging requirements – many types of miniature or Nano equipment will perform satisfactorily with low harvested power. In this thesis, to generate the required power that will perform a satisfactory job of charging our target device or application (UAVs), the focus will be placed on harvesting significant energy.

3. SYSTEM MODEL

This chapter will discuss: The system description, and the formulae used to derive the proposed model.

3.1 SYSTEM DESCRIPTION

With the sources of the energies identified, the next step is to consider the setup of the receivers for the harvested energy. Note that a unit harvesting source can only yield the same amount of energy that will be sufficient to charge the storage banks. The concept of the receivers will be discussed here, in terms of radiative and inductive power receptions.

3.1.1 Radiative Far/Near Field Reception

3.1.1.1 Antenna array

A receiver antenna is used to receive (attract) the transmitted frequency. The model will propose an array of directional antennas with high gain, which will receive frequencies from different sources available. Then, all the source outputs are aggregated to produce a high level of power. Within this array will be antennas of different RF bands, depending on the channels available for harvesting. The received frequencies of different bands are sent through different Rectenna blocks for conversion.

3.1.1.2 Rectenna

Received high frequency RF waves need to be converted to electrical energy. This is done with the use of rectenna [28]. A rectenna consists of dipole antennas connected to dipole elements (Schottky diodes) through filters [29], as seen in Fig. 3.1. The Schottky diodes have a wide tolerance for high frequency switching without losing much power in the form of drop voltages. Additionally, they don't break down due to overheating. These diodes convert the incoming high frequencies into low DC voltages, depending on the received power of the RF wave. The converted voltage is then smoothed or filtered by capacitors. The circuit can be expanded, depending on the desired output voltage level, using the *nth* staged voltage doubling element.

3.1.1.3 Regulator

At the regulator stage, a constant value for voltage is to be maintained at the output of all the received, rectified, and filtered DC voltages from the rectenna blocks. This is achieved with the use of voltage regulators. It is after this level that all the individual power components of the antenna array are aggregated to increase the overall power level at its output.

Super capacitors have the ability to charge quickly and store a tremendous amount of energy. Therefore, integrating super capacitors (500F) into the drone system will allow the unit to be charged quickly, as well as filtering any spikes or ripples that occur during charging.

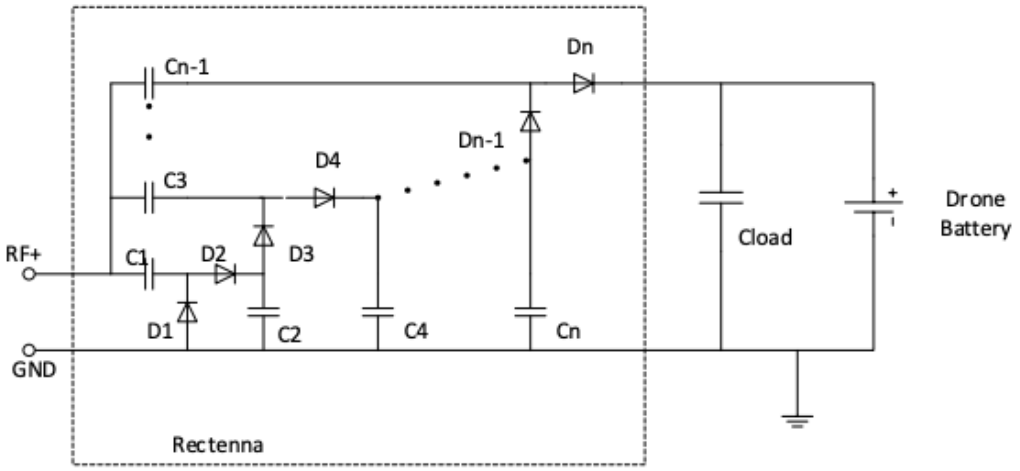

Figure 3.1: Schematic Showing the Rectenna circuit consisting of an N-Stage Cockcroft-Walton Charge Pump (Voltage Multiplier)

Thus, the system of the RF WPT will be as illustrated in Fig. 3.2. The number and types of antennas to be used will depend on the frequency available in the deployment space. There will be directional antennas placed at different tilt angles facing the source of strong signals.

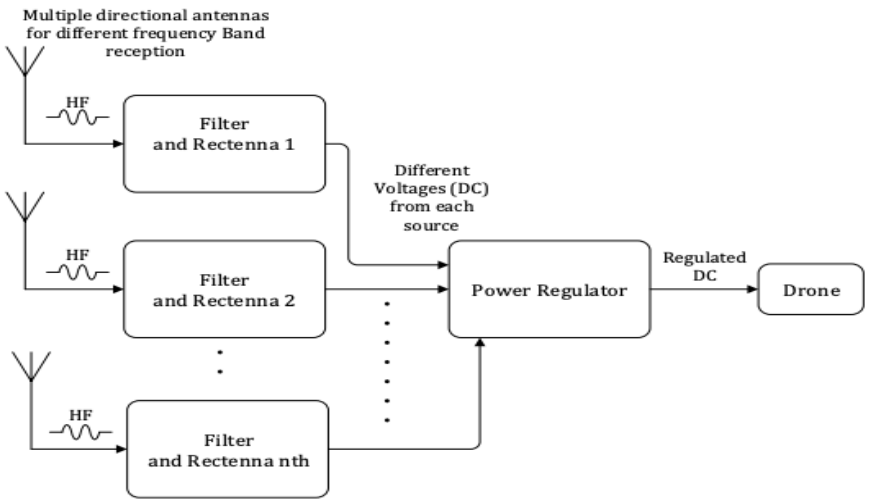

Figure 3.2: Diagram showing the RF harvesting blocks from the multiple frequency, different direction reception antennas, to the charging phase

3.1.2 Inductive Power Reception

Inductive power is obtained from the transfer of energy through induction over close distances and a strong electric field. However, for this to be viable for the proposed model, the distance D for such a transfer will have to be larger, because the receiver will be placed at a considerable safe distance to the UHVTL.

Based on the components of induction, experimental works carried out on live UHVTLs by Luo et al. in [25], provide several backgrounds and scenarios to test for these theories on induced voltage on a given line (let's call it S). In the results of their work, they highlighted three important facts. The induced voltage in S;

- increased as the length of the transmission line increased. The referenced distance was from 500m to 10km.
- decreased as the distance of separation between S and the UHVTLs increased. The referenced distance was from 45m to 90m.

- increased as the distance between S and the ground increased. The referenced distance was 20m to 140m from ground level. However, it experienced a sharp drop at the middle phase line. This drop was due to the upper and lower line force fields cancelling out their force field rather than increasing the resultant field.

With these three points, a base can be established on the design of the proposed model. To achieve an efficient system that will supply significant power, the model will consider the distance variation as reference for the design.

Most of power obtained for energy transfer through induction is done over a close distance and a strong field. Here, using the transformer principles, the UHVTL represents the primary side of an isolation transformer. It generates high voltage and a reasonably high current. In terms of winding length and density, there are several parallel lines running a distance of several kilometers at different phases. On the secondary side will be a coil winding on a core. The core size and winding turns will be determined by the amount of voltage or current required, taking into consideration isolation gaps between the primary (UHVTLs) and the secondary winding. Fig. 3.3 shows a representation of the system coupling.

3.1.2.1 The Coil

It is a coil winding on an iron core, which will lay parallel to the UHVTL over a relatively strong magnetic field.

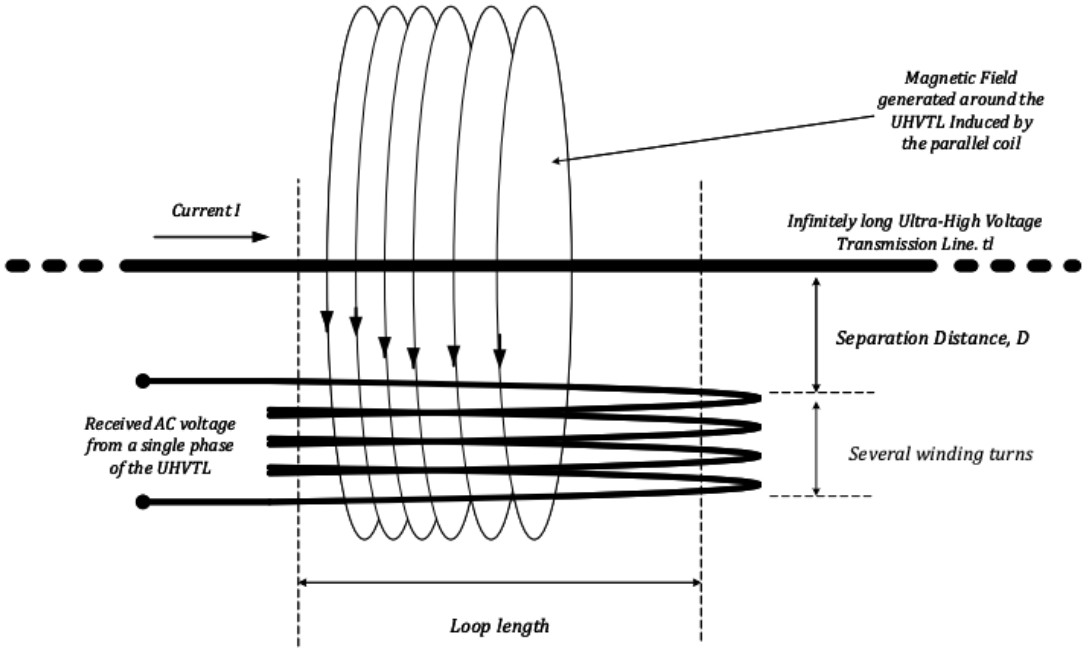

Figure 3.3: Magnetic Field generated around a UHVTL that induces current in a parallel coil

The proposed system will make use of an existing UHVTL, which is commonly located between the generating source and distribution settlements. The induction coil must be placed in close proximity to strong fields of the UHVTLs to induce power. In our case, it will be mounted on the UAV. Because this power is in low AC form, it is passed through a Cockcroft Walton voltage doubler. This is a regulator block to maintain constant voltage. Then, it's passed to a current doubler circuit that will cut the voltage in half and double the current. Finally, the rectified power is used to charge the UAV. There is a need for more winding wires to give a reasonable charging output to feed to the accumulators, but this will increase in overall weight of the coil unit. This model is seen in Fig. 3.4.

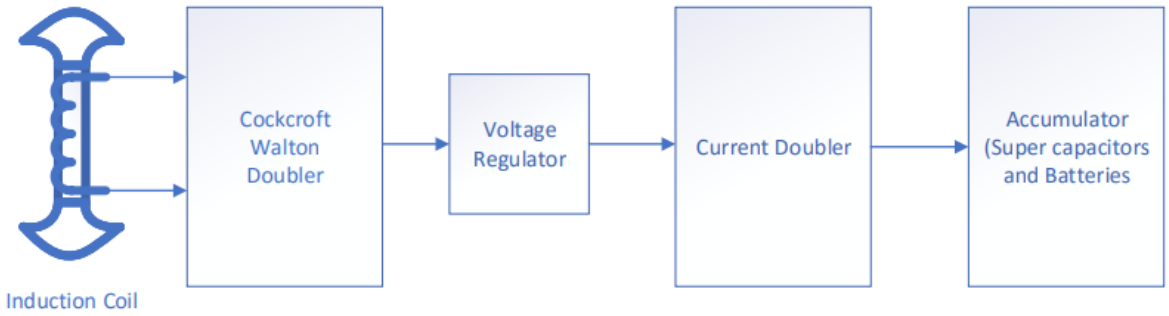

Figure 3.4: A Flow diagram showing a detailed layout of the system, from input induction source to UAV battery unit.

3.2 FORMULATION

3.2.1 Wireless Energy Harvesting from BTS

For this sequence to be successful, calculations for the electromagnetic wave transmission are crucial.

Let's consider the electromagnetic wave propagation. Electromagnetic waves are components of electric and magnetic waves, as the name implies. They are transmitted perpendicular to each other. The total power carried by these waves in Far Field are expressed by a Poynting equation:

$$\bar{P} = Re(\bar{E} \times \bar{H}^*) \quad (W/m^2) \tag{3.1}$$

Where

E – Is the electric field intensity (V/m)

H – Is the magnetic field intensity (A/m)

Re – Is the real part of the equation and,

Asterisk (*) - Is the complex conjugate part of which both E and H are a quantity.

Power density as observed at a point distance R from the source (sphere) is expressed as:

Where $\eta_o = 377\Omega$ is the intrinsic impedance of free space.

$$P = \frac{E^2}{\eta_o}(4\pi R^2) \quad (W) \tag{3.2}$$

Also, the relationship between E and H is

$$\eta_o = \frac{E}{H} \qquad (\Omega) \tag{3.3}$$

Now the power density P_d that is received from a transmission antenna at a distance is expressed as,

$$P_d = \frac{P_t G_t L_t}{4\pi R^2} \quad (W/m^2) \tag{3.4}$$

Where

P_t – Power transmitted (W),

G_t – Gain of the transmitting antenna,

L_t – Transmission line loss,

R – Distance between the transmitting and receiving antenna (m).

As also derived by Liao [30] from field theory, considering far field and a free space medium.

$$P_d = \frac{E^2}{\eta_o} = \frac{E^2}{120\pi} \quad (W/m^2) \tag{3.5}$$

Therefore, field intensity can be derived from Eq. (3.4) and (3.5) to be

$$E = \sqrt{120\pi P_d} = 19.4\sqrt{P_d}$$

$$= \frac{5.48}{R}\sqrt{P_t G_t L_t} \quad (V/m) \tag{3.6}$$

Also for;

$$Receiving\ Antenna\ Factor\ (AF) = \frac{E}{V} = 19.8 - 20log_{10}(\lambda) - G_r \quad (dB) \tag{3.7}$$

Where

λ – The wavelength of the transmitting frequency(m),

G_r – Gain of the receiving antenna (dB).

Establishing the formulae that relates all the components which brings power to the receiving antenna, there is little we can do to change most of the parameters because, we don't dictate to the BTS operators how to propagate their resources. However, what is of great importance to us here is knowing our maximum possible effective distance from the transmission point.

The distance between transmitter and receiver (or radius) represented by R differs depending on the type of transmission power targeted. It depends on the frequency band from which the energy will be harvested.

For the Far Field – also known as the Fraunhofer region, the effective distance R_F of the receiver antenna from the BTS is expressed as

$$R_F = \frac{2D^2}{\lambda} \quad (m) \tag{3.8}$$

Where

D – Is the diameter of the receiver's antenna (m^2),

λ – Is the wavelength of the propagation wave(m).

Then, for the reactive Near Field region, the effective distance R_N of the receiver antenna from the BTS is expressed as

$$R_N = 0.62\sqrt{\frac{D^3}{\lambda}} \quad (m) \tag{3.9}$$

However, the formula for the radiating near field, also known as the Fresnel region, is the same as that of the Far Field propagation.

At the Rectenna, the energy coverage radius R_E is given as

$$R_E = \sqrt{\frac{1}{S}P_t G_t G_r \left(\frac{\lambda}{4\pi}\right)} \quad (m) \tag{3.10}$$

Where S is the rectifier sensitivity.

Rectenna's diode cut-off frequency f is expressed as

$$f = \frac{1}{2\pi R_s C_j} \quad (Hz) \tag{3.11}$$

Where

R_s – The diode's series resistance

C_j – Zero-bias junction capacitance

Because most of the quantities we will be dealing with are in the dimensions of two power level ratios, which is decibel dB, we will highlight the formula for these conversions. This is expressed as

$$dB = 10log_{10}\left(\frac{P_2}{P_1}\right) \tag{3.12}$$

P_2 is the power level with respect to a reference power P_1 – which, in most cases is equal to 1

When the decibel value is above $1W$ it is expressed as dBW. When the value of the decibel is above $1mW$ it is expressed as dBm. The relationship between the dBW and dBm is given as

$$dBW = -30 + dBm \tag{3.13}$$

Then, in terms of the received power P_r – given that the parameters are in dB and the transmitted power is in dBW – the expression is

$$P_r = P_t + G_t + G_r - L_t - L_r - 20log_{10}\left(\frac{4\pi R}{\lambda}\right) \quad (dBW) \tag{3.14}$$

Where L_r is the receiving antenna loss (in this case, with the unit of dB).

For free space loss (FSL) received power P_r is expressed (in dBm) as

$$P_r = P_t + G_t + G_r - FSL \qquad (dBm) \tag{3.15}$$

And FSL from Eq. (3.15) is expressed in terms of distance and propagation frequency as

$$FSL = 32.45 + 20log_{10}(d_{km}f_{MHz}) \qquad (dBm) \tag{3.16}$$

Where

d_{km} – The distance between the transmitter and receiver antennas (km)

f_{MHz} – The transmitting frequency (MHz)

And in terms of ***transmitting*** power density

$$P_d = -11dB - 20log_{10}R + P_t + G_t - L_t \quad (dBW/m^2) \tag{3.17}$$

While for ***receiving*** power density

$$P_d = 11dB - 20log_{10}\lambda + P_r - G_r - L_r \qquad (dBW/m^2) \tag{3.18}$$

With these equations, we can now run our analysis to see what amount of power we can receive at any good proximity between base transceiver station (BTS) coverage areas.

3.2.2 Energy Harvesting from High Voltage Transmission Lines

For energy harvesting from Ultra-High Voltage Transmission Lines (UHVTL), the basic principles of electromagnetic induction states that any current carrying conductor of a given length generates a magnetic field around it. This force field is perpendicular to the direction of flow of the current. When a conductor is introduced into a magnetic field, a current is induced due to the change in magnetic flux on the electron particles in the conductor. The strength of such power transfer depends on the strength of the field, the flux transfer medium, and the conductor or coil form factor.

Let's consider two parallel transmission lines of length l, separated by a distance r and carrying currents I_1 and I_2 , which are flowing in the same direction. This is illustrated in Fig. 3.5.

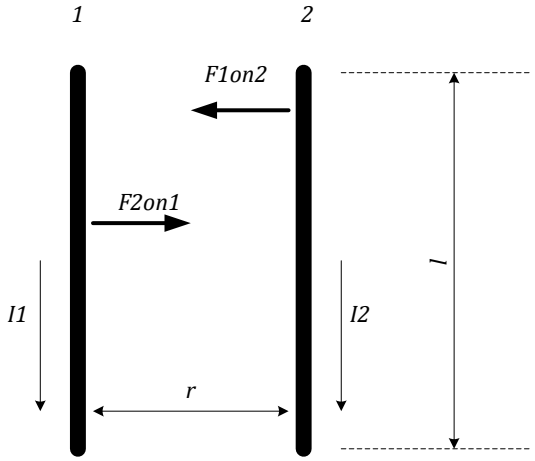

Figure 3.5: Magnetic Force field between two current carrying conductors

The force field in the conductor 1 will be

$$F_1 = B_2 I_1 l \quad (N) \tag{3.19}$$

Where

B_2 – Magnetic field generated by the conductor 2

But,

$$B_2 = \frac{\mu_0 I_2}{2\pi r} \quad (T) \tag{3.20}$$

Therefore substituting for B_2 in Eq. (3.19)

$$F_1 = \frac{\mu_0 I_2 I_1 l}{2\pi r} \quad (N) \tag{3.21}$$

Based on Newton's law, the force field in the conductor 2 with respect to the magnetic field in conductor 1 will be

$$F_2 = \frac{\mu_0 I_1 I_2 l}{2\pi r} \quad (N)$$

$$F_1 = F_2 \tag{3.22}$$

The magnetic flux is the area through which the magnetic field is cut, expressed as

$$\Phi = BA \quad (Tm^2) \tag{3.23}$$

Where A is the area through which the field cuts.

Faraday and Len's Law expresses the induced emf in any coil that lays in the field as

$$E = -N\frac{\Delta\Phi}{\Delta t} \qquad (V) \tag{3.24}$$

Where N is the number of turns of the conducting coil. The minus sign is Len's Law, which states that motion must cut across the field for emf to be generated.

The induced emf can be expressed with respect to the area by substituting Eq. (3.23) into Eq. (3.24) as

$$E = -NA\frac{\Delta B}{\Delta t} \qquad (V) \tag{3.25}$$

The emf in terms of current i and inductance L (Appendix A) is expressed as

$$E = -L\frac{\Delta i}{\Delta t} \qquad (V) \tag{3.26}$$

The inductance in terms of coil diameter and core radius is

$$L = \frac{\mu_0}{\pi}\left[ln\left(\frac{d}{r}\right) + \frac{1}{4}\right] = \frac{\Phi}{i} \qquad \left(\frac{Tm^2}{A} or\ H\right) \tag{3.27}$$

Where

d – Is the distance of the coil loop,

r – Is the radius of the coil, and

μ_0 – Is the magnetic permeability of free space expressed as 4×10^{-7}

This proves that when the currents in the conductors flow in opposite directions with the same magnitude, their force fields cancel each other out, giving a resultant zero.

There are two main ways through which induction can happen between two transmission lines running parallel or at an angle to each other, as discussed in [24]. The first is through electrostatic induction through capacitive coupling. The second is electromagnetic induction through mutual inductance [31].

The capacitive coupling (electrostatic induction) method is dependent on the capacitive properties created by the medium separating the lines from each other and the ground. It is not dependent on the distance of separation between the lines [32]. Fig. 3.6 shows an illustration of the effect of capacitive coupling on transmission lines.

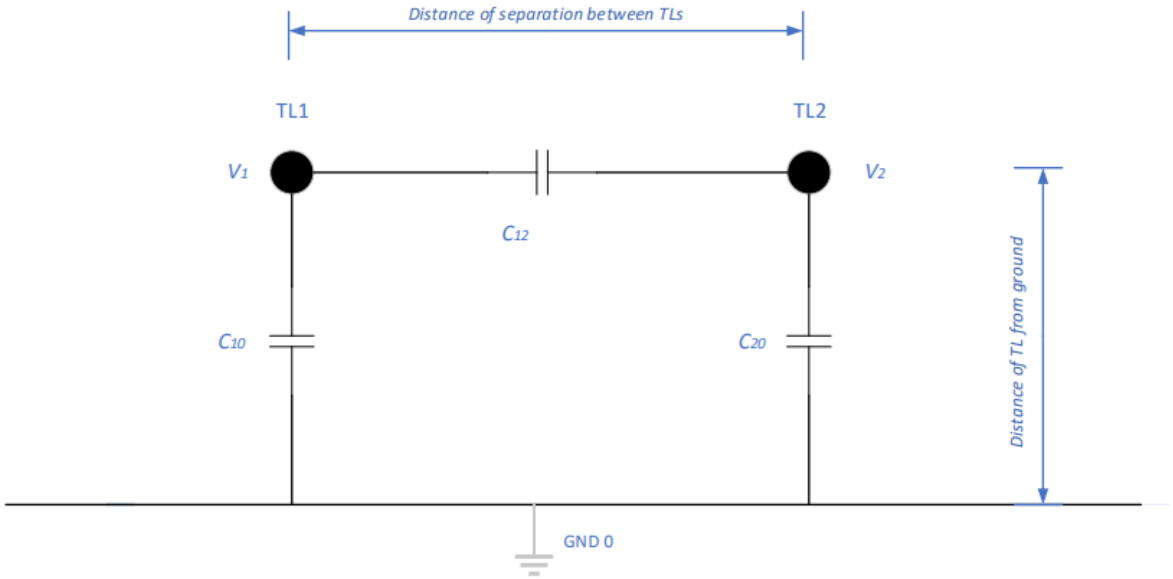

Figure 3.6: Presence of capacitive coupling acting on transmission lines

From Fig. 3.6, the formula for voltage V_2 induced in the transmission line 2 (TL2) due to the transmission line 1 (TL1) is

$$V_2 = \left(\frac{C_{12}}{C_{12}+C_{20}}\right) V_1 \quad (V) \tag{3.28}$$

Where,

V_1 – High voltage transmitted on the transmission line

C_{12} – Capacitance between TL1 and TL2

C_{20} – Capacitance between TL2 and ground

However, the capacitive coupling effect is greatest on TL2 when both ends of TL2 are open (not grounded), as we will demonstrate shortly.

In the case of the mutual induction coupling (Electromagnetic Induction), the distance of separation between the two TL and the ground play a vital role in the induced voltage on the TL2. Let's discuss the effect of the distance of separation between the transmission lines as it relates to the voltage induced in the case of parallel running TLs, separated by certain distances.

Assume an infinitely long UHVTL, $tl.$ is placed at a distance from other conductors of the same diameter (1, 2, 3, …, n),carrying their respective currents and running parallel to each other. This is shown in Fig. 3.7.

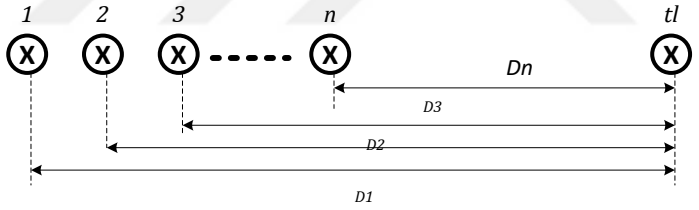

Figure 3.7: Cross-sectional view of parallel conductors showing their relationship with respect to their distance. The Current direction is into the paper.

The resulting magnetic flux linkage λ generated by the three lines with respect to the conductor as derived in [31] is expressed as:

$$\lambda_{tl} = 2 \times 10^{-7}\left(I_1 ln\left(\frac{1}{D_1}\right) + I_2 ln\left(\frac{1}{D_2}\right) + I_3 ln\left(\frac{1}{D_3}\right) + \cdots + I_n ln\left(\frac{1}{D_n}\right)\right) \quad (Wb - turn/m) \tag{3.29}$$

Where

D – Represents the respective distances of all the conductors from the TL, in terms of their individual subscripts.

From the flux linkage equation, we can now obtain the voltage induced in the TL as

$$V_{tl} = j\omega\lambda_{tl} \quad (V/m) \tag{3.30}$$

Where $\omega = 2\pi f$ is the resonance frequency.

This is the voltage due to mutual inductance between the powered transmission line and the energized transmission line tl. In this thesis, the energized line will be a coil.

This gives us the voltage on the transmission line with respect to the collective conductors. When there are more tl that are insulated and closely packed together to form conductors $tl_1, tl_2, tl_3, \ldots tl_n$, each of them will have an induced voltage as expressed in Eq. (3.30).

In this thesis, we will not attempt to curb or merely measure the effect of these induced voltages on the transmission lines. The concern is not how far our induced line will go, but how to harvest energy that can be used to charge drones. To put this theory into practice, I proposed a coil winding design that will create a huge isolation type, voltage stepdown transformer.

Since windings are now involved, the transformation formula will play a big role in getting the system to accumulate the power that necessary for charging. We will use the well-known transformer relationship, which is expressed as

$$\frac{N_p}{N_s} = \frac{V_p}{V_s} = \frac{I_s}{I_p} \tag{3.31}$$

Where,

N_p – Number of turns of the primary coil

N_s – Number of turns of the secondary coil

V_p – Voltage on the primary side of the transformer

V_s – Voltage on the secondary side of the transformer

I_s – Current on the primary side of the transformer

I_s – Current on the secondary side of the transformer

From this relationship, we can easily deduce that an increase in the number of coil turns results in an increase in voltage (because of the direct proportionality), and a decrease to the current on the resulting side. Therefore, all of the factors from V_{tl} per meter, including the wire gauge based on the desired current and the core type, will decide the overall parameter for the coil design with reference to an existing input parameter. Other formulas that are used to get the results in this thesis are listed in Appendix A.

When current I is flowing through a coil placed in a magnetic field, and this coil has the resistive value R with an inductance L, as shown in Fig. 3.8:

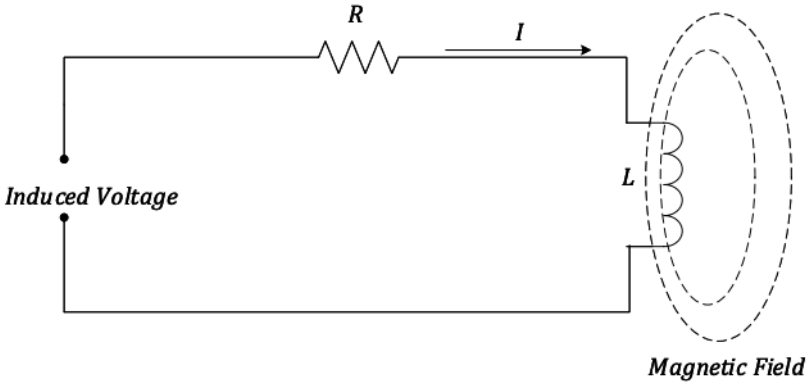

Figure 3.8: An inductive Circuit

The induced voltage is expressed as

$$V = I\sqrt{\omega L^2 + R^2} \qquad (V) \tag{3.32}$$

Where $\omega = 2\pi f$

For a solenoid coil having a core length of L, with N numbers of winding turns carrying a current I, the magnetic field concentration in the uniform field is expressed as,

$$B = \mu I \frac{N}{L} \qquad (T) \tag{3.32}$$

Where μ is the permeability, which is the product of relative permeability of the core material μ_r and absolute permeability $\mu_0 = 4\pi \times 10^{-7}$. The relationship in (3.32) will be used to determine the current that is induced in the coil design after measuring the concentration of magnetic flux within the core.

4. ANALYSIS AND RESULTS

4.1 RF ENERGY HARVESTING

An analysis was carried out using transmission parameters as obtained in Table 4.1. The analysis assumes that the available 3G and 4G frequency bands are 2.1GHz and 2.6GHz respectively.

Table 4.1: Simulation parameter for RF energy harvest

Parameter	**Value**
Transmitting Power (P_t)	50dBm
RF band	2.1GHz and 2.6GHz
Transmitting Antenna Gain (G_t)	20dBi
Receiver Antenna Gain (G_r)	25dBi

A characteristic chart, as seen in Fig. 4.1, is obtained from the given input parameter in Table 4.1, at 2.1GHz band.

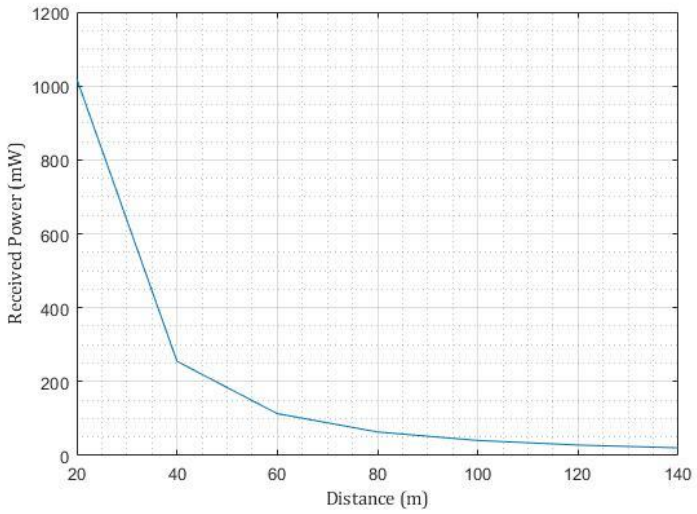

Figure 4.1: Plot of received power vs distance between transmitting and receiving antenna

Table 4.2: Result showing received power at different distance ranges for two separate considered frequency bands

Distance (m)	**Received Power (Watts)**	
	2.1GHz	2.6GHz
20	1.0198	0.6652
40	0.2549	0.1663
60	0.1133	0.0739
80	0.0637	0.0275
100	0.0408	0.0177
120	0.0283	0.0122
140	0.0208	0.0090

As shown in Table 4.2, more power is obtained at higher power levels with a lower RF band. As the distance from the transmitting station increases, the power level drops. A 25dBi receiver directional antenna may sound farfetched, but in time, it will be readily available. To achieve significantly useful energy delivery for charging, our calculations will determine the locations of the receiver antennas with respect to their respective energy sources. We will run the values of a typical BTS transmission frequency and check it against the received power level with respect to their distances apart.

In a 3G setup, the number of Base Transceiver Stations (BTS) in a square kilometer is generally 4 or 5. In the case of a 4G (LTE) topology, the number rises to about 8 to 10 BTS per km^2. Given this information, the best location to position antennas in these clusters, will be based on mobile cell optimization and frequency bands. Suitable distance is matched to frequencies, and their desired results is as expressed in Table 4.3.

Table 4.3: Estimated power harvested from a given scenario

Distance From BTS (meters)	Calculated received power at given distance (Watts)	Numbers of directional antennas	Total power generated (Watts)
80 (for 2.1GHz)	0.0637	5	0.3185
40 (for 4G)	0.1663	5	0.8315
Total Power Harvested			**1.1500**

10 of these antennas locked in the direction of their respective target frequency bands would harvest about 1.15W of power from the surrounding BTS. This power is fed to the rectenna voltage doubling circuit, which pre-charges it through boost rectification.

4.2 UHVTL ENERGY HARVESTING

For the UHVTL, we used an electromagnetic field simulation software for transmission lines known as QuickField. The software was used to carry out the simulations for both magnetic field components (AC magnetics analysis) and electric field components (AC conduction analysis).

The parameters used in the simulation scenario are two three phase UHVTLs running on transmission towers with dimensions as shown in Fig. 4.2. Each transmission line is carrying voltages of 100kV and a current of 500A, running parallel to each other through a distance of 1km.

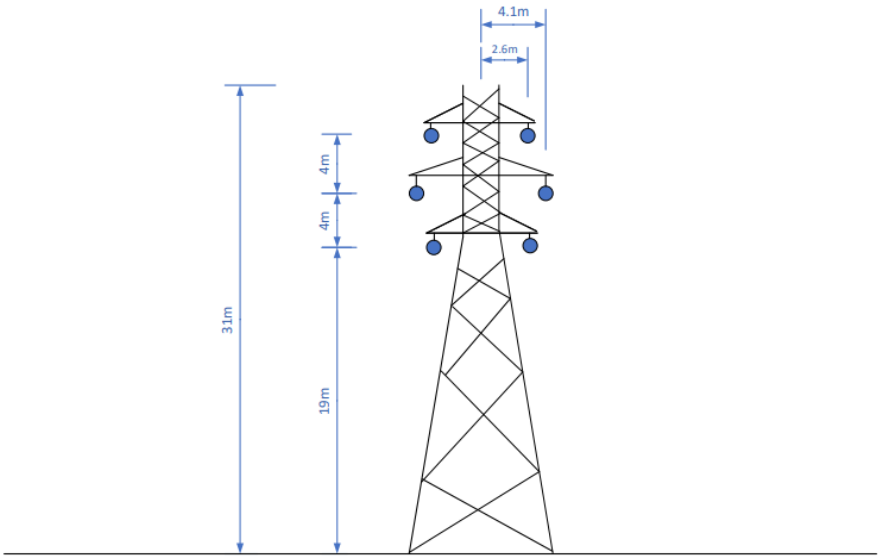

Figure 4.2: Dimension of the simulated UHVTL tower showing the 3 x 2 transmission cables hanging from their insulators.

The fields generated around the transmission lines in the simulations are as seen in Fig. 4.3 to Fig. 4.6. Only the effective field portions are shown in the plots of Color Maps and Isolines. As observed, the field is strongest close to the conductor clusters. But the isolines show the projection of a stronger energy vertically upward as compared to other directions, in the cases of the AC Conduction, but almost horizontally symmetrical in the AC Magnetics. This is the same when applied in a downward direction, due to the earth's magnetism).

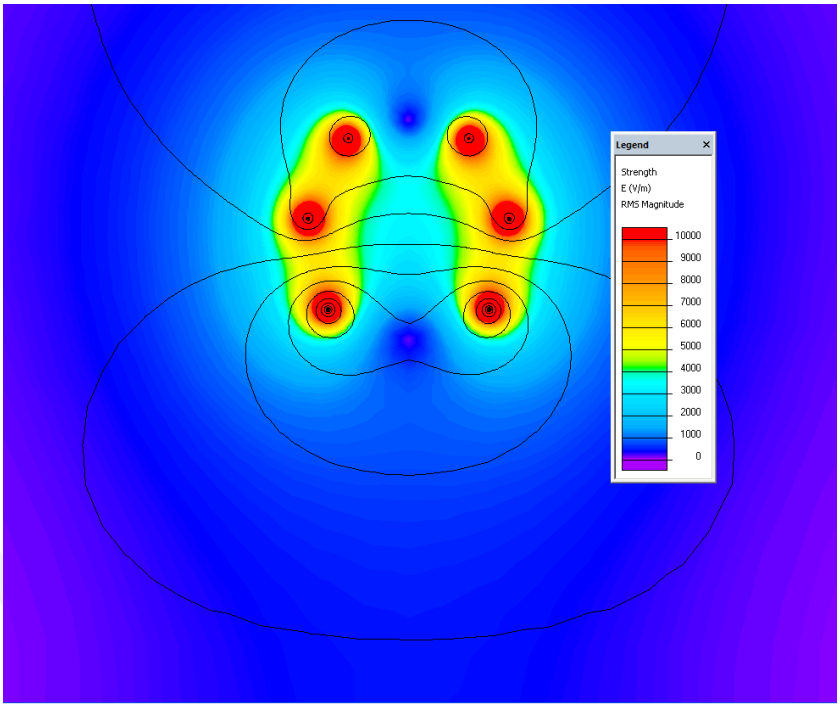

Figure 4.3: AC conduction simulation results showing the six transmission cables and the effective electric fields strength formed around them (simulation was performed using actual scale)

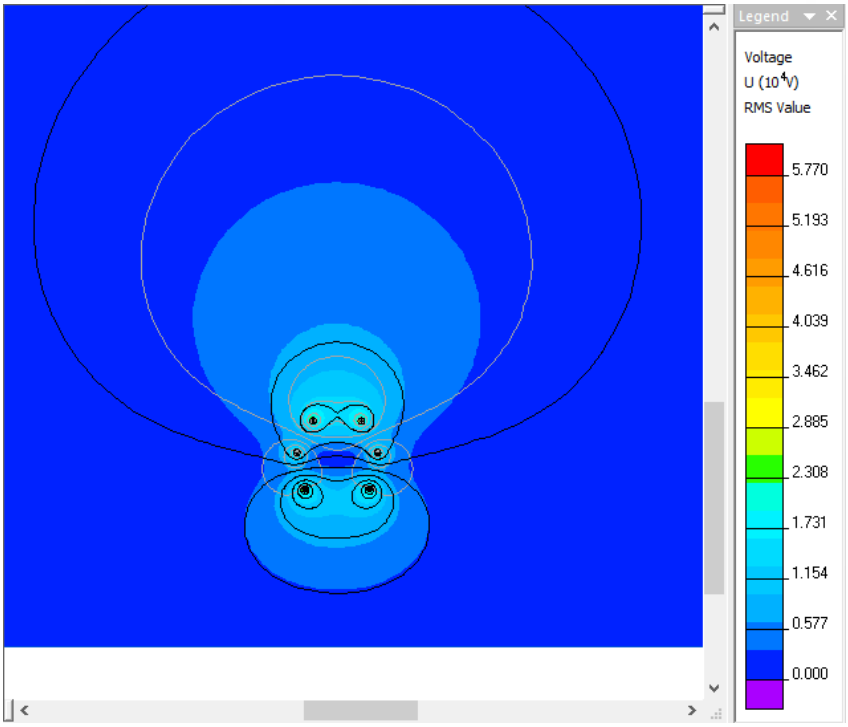

Figure 4.4: AC Conduction simulation showing resultant floating voltage around transmission lines

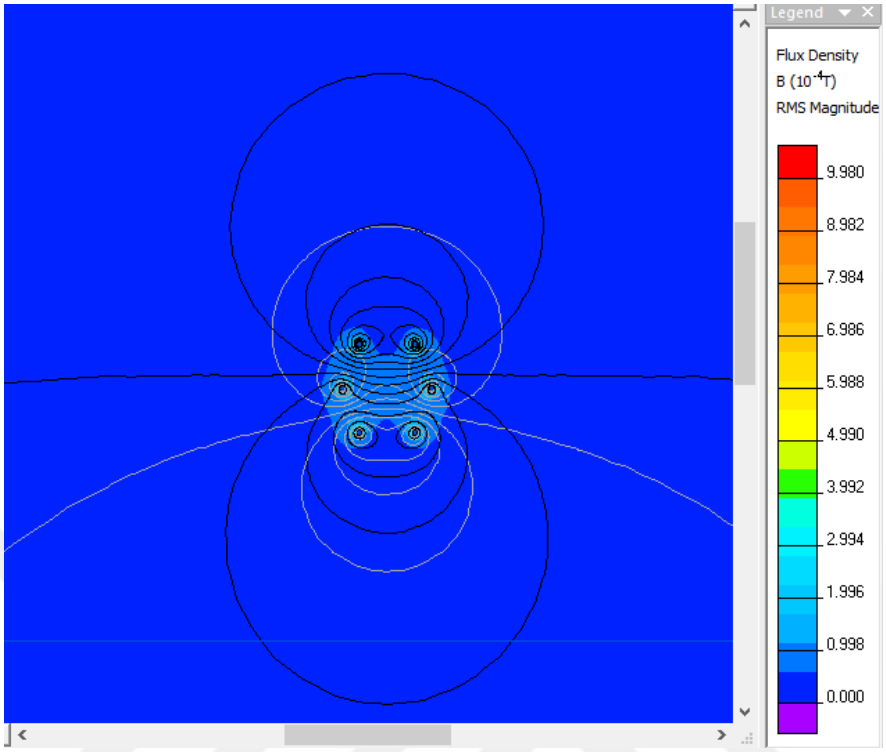

Figure 4.5: AC Magnetic analysis showing the magnetic flux density around transmission lines

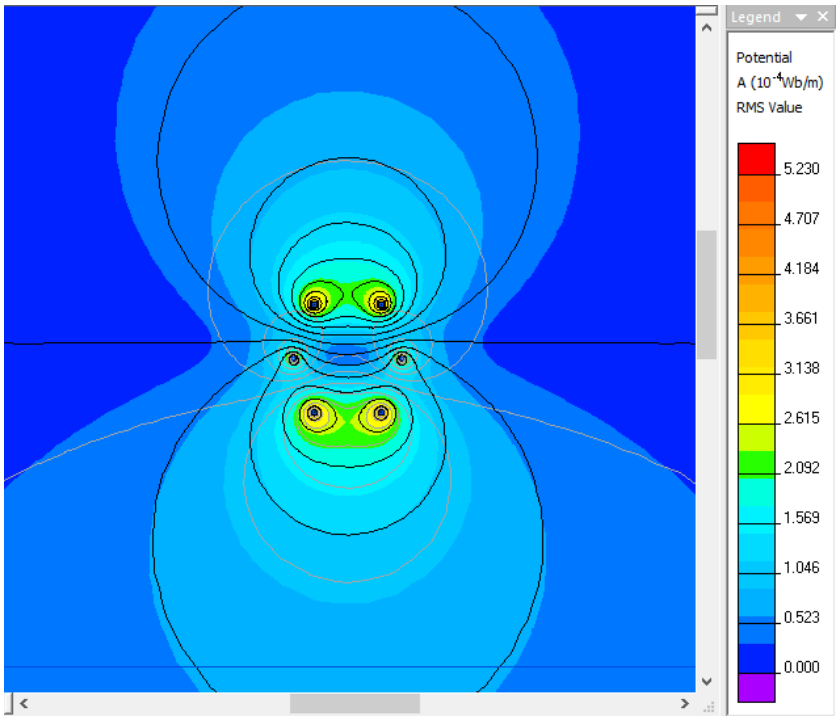

Figure 4.6: AC Magnetic analysis showing an instance capture of the magnetic field's potential radiation around the transmission lines

Furthermore, these simulation results are analyzed at two vertical cross-sectional points of the transmission lines. A cross-section plane is taken at the symmetrical center of the transmission tower, cutting from the zero potential ground level to beyond the height of the tower (31 meters). This measures the numerical values of the fields through a chart. Then, a vertical cross-section from a horizontal distance of 10 meters from the symmetrical center of the tower is taken, which also starts from ground level and reaches beyond the tower height. It is noticed that field strength is at its peak overhead the powerlines, and reduces the closer you get to ground level.

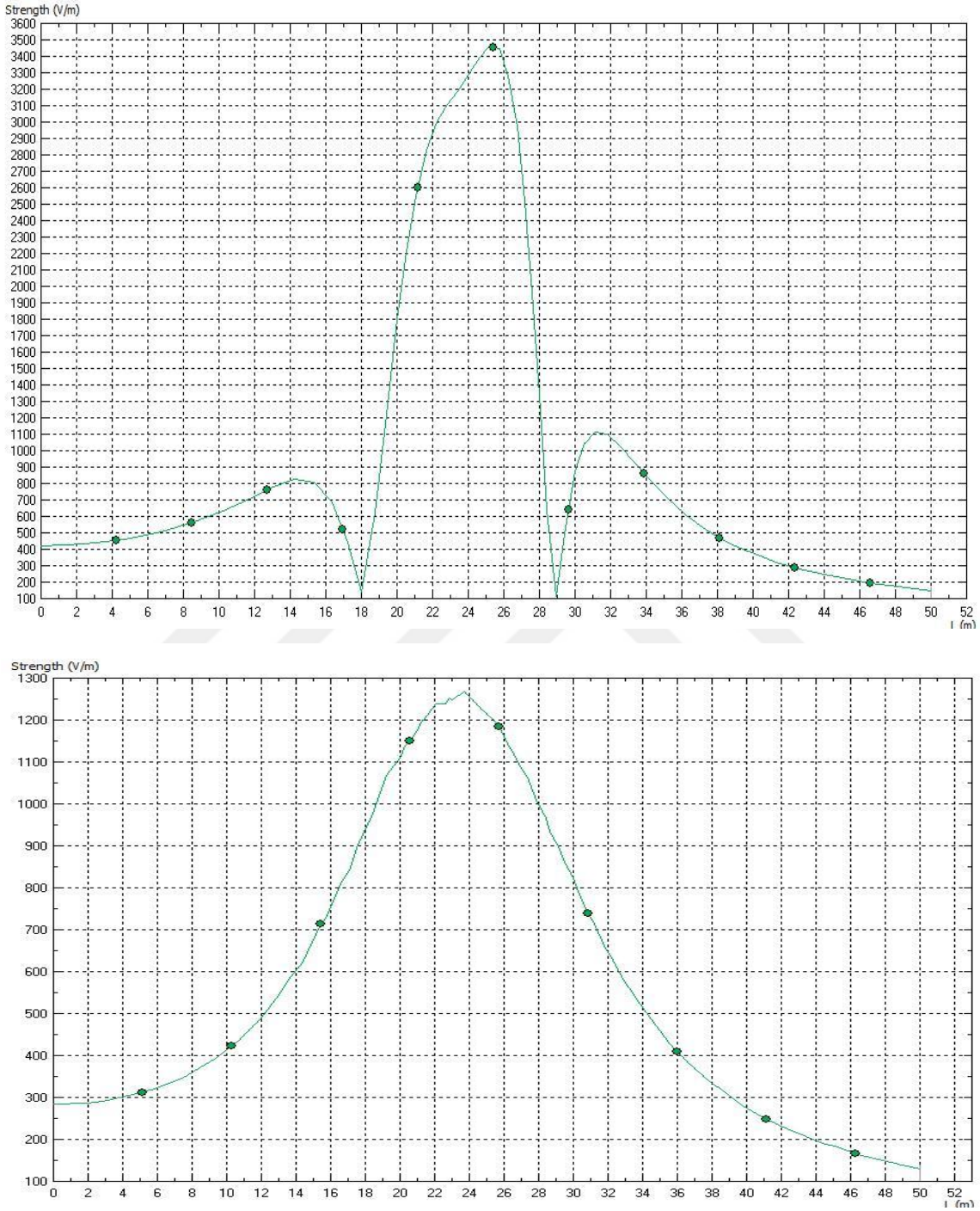

Figure 4.7: AC Conduction plot of electric field strength from cross-section taken: (Top) at the symmetrical center, and (Bottom) 10 meters away from the center of transmission tower

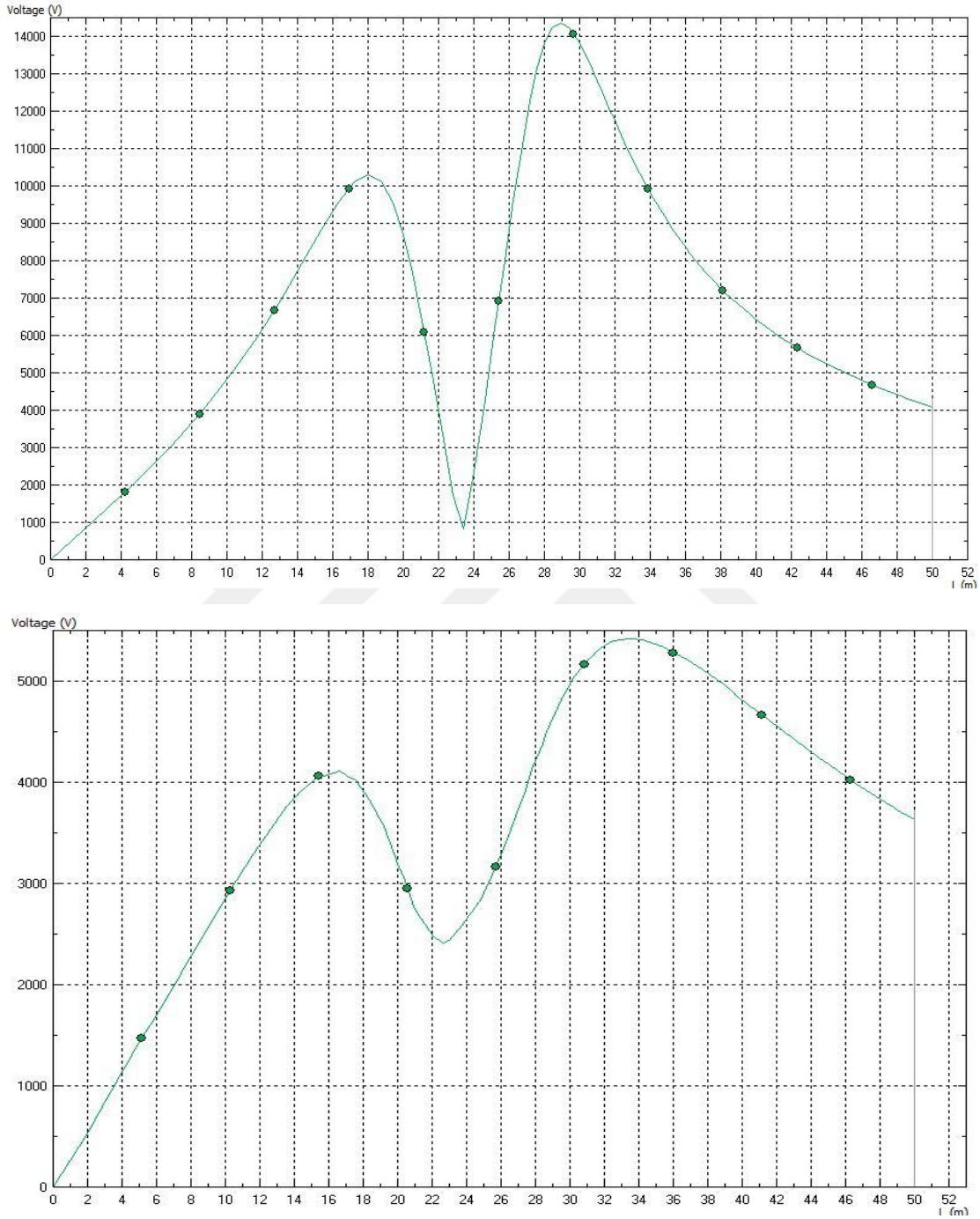

Figure 4.8: Floating voltage around the transmission line plot taken from the: (Top) symmetrical center, and (Bottom) 10 meters from center of the tower's reference point

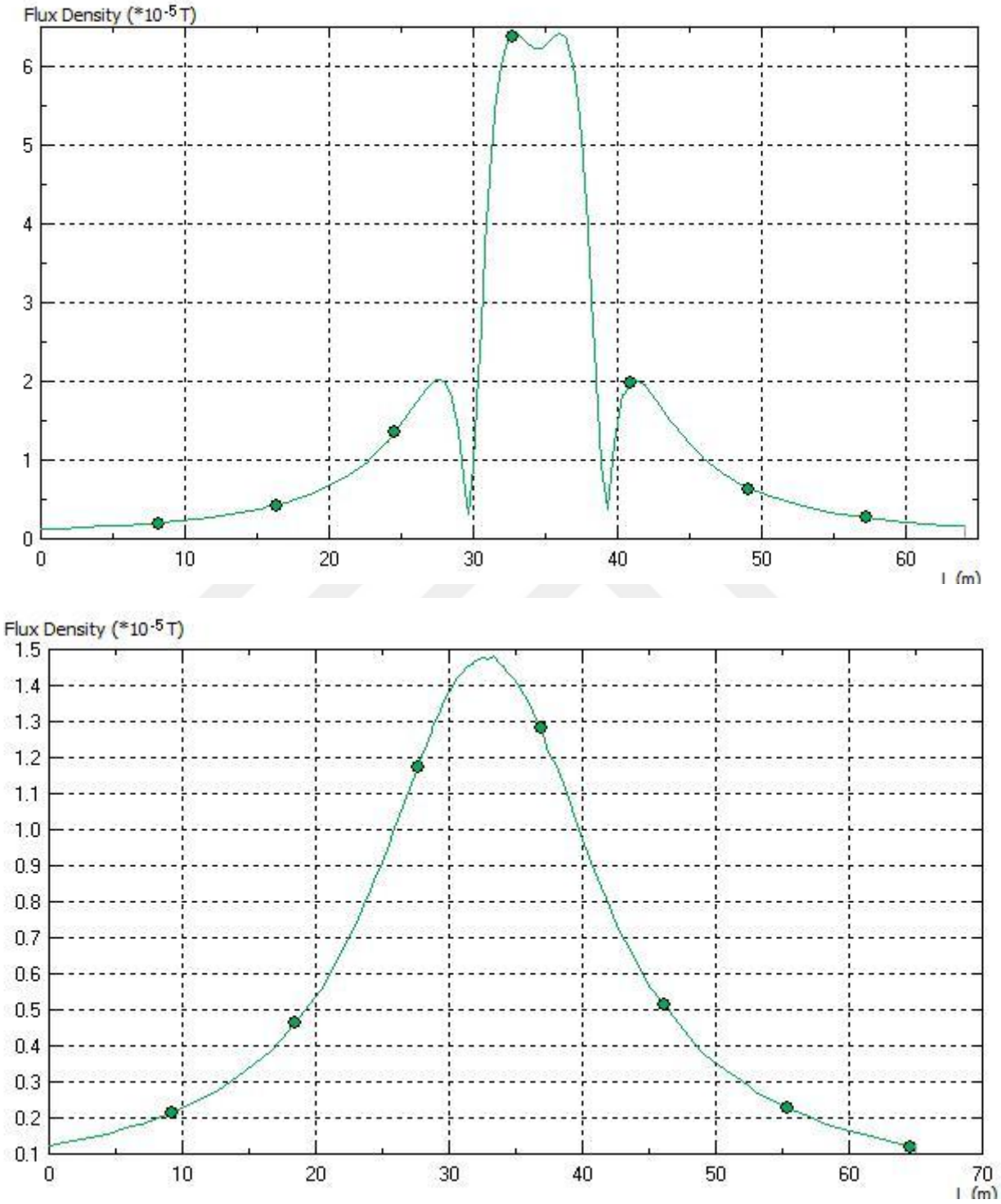

Figure 4.9: Magnetic flux density around transmission line plot taken from the: (Top) symmetrical center, and (Bottom) 10 meters from center of the tower's reference point

From our analysis, as seen in Fig. 4.7 to Fig. 4.9, it is clear that the strongest fields exist at the symmetrical center of the UHVTL. This means that for the best harvest results, the induction coil must hang under or in-between the overhead ultra-high voltage power lines. This leads us to consider the hazards and impracticality involved in the deployment of this solution. However, in the case of a hovering vehicle such as a drone, the resultant peak of all the fields is observed at a height of about 28 – 30 meters, right above the transmission tower. This is because that field is far from the ground, and yet closer to the transmission lines. Therefore, mounting a charging coil in a drone that will hover at such height above the UHVTLs will generate sufficient power to charge the drone.

4.2.1 Coil Model

Research by Yuan et al. [2] into the harvest of energy from UHVTL using coils proposes a Bow-Tie Coil model. This model was able to generate 146.7mW power in a $11\mu T$ magnetic field. Their coil performed much better than the one proposed by Roscoe et al. in [1], in which a solenoid coil is designed to harvest energy for the use of a low power dependent sensor.

Having considered the recommendations to improve the result achieved by the Bow-tie coil, I propose an improved modification which would build more Magnetic Flux density with the coil. Fig. 4.10 shows the designs of the winding cores.

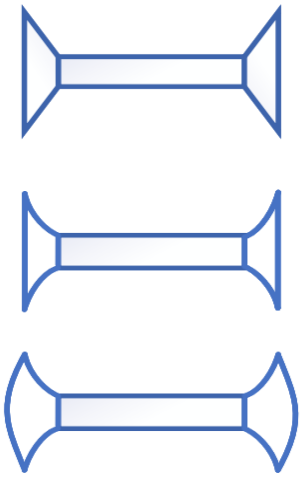

Figure 4.10: Yuan et al. Bow-tie Coil (Top), our first modification to the Bow-tie Coil model (center), Curved Core Design (bottom)

[2] also state the concerns of proximity of the coil, which is impeded by the practical distance that the coil can be placed from the harvesting source. In their case, the coil was placed at a distance of 5 meters above ground level. Because our design seeks to harvest energy in order to charge hovering UAVs, these UAVs can hover at a closer proximity to the power lines, such as the top height of about 40m where the magnetic flux field is strongest. This is seen in Fig. 4.9. It will also go a long way in reducing the size of the harvesting coil, which will make it able to fit on the UAV. Because the core material will play a major factor in terms of weight and performance [33], I chose to use a Silicon Core Iron B (SiFEB) alloy for the analysis. The presence of Silicon in the steel material decreases the resistivity of the iron, which means a lower Eddy current and a narrow loop for Hysteresis. This reduces the overall core losses. The volume density of the Silicon Core Iron alloy is $7650kg/m^3$, with a relative permeability of 1500 [34].

I used Comsol Multiphysics to create a Helmholtz coil, which was used to generate a Magnetic Flux Density similar to our UHVTL environment. Between the Helmholtz coils we placed different core designs. The generated magnetic flux concentration in the core materials are seen in fig. 4.11-4.13

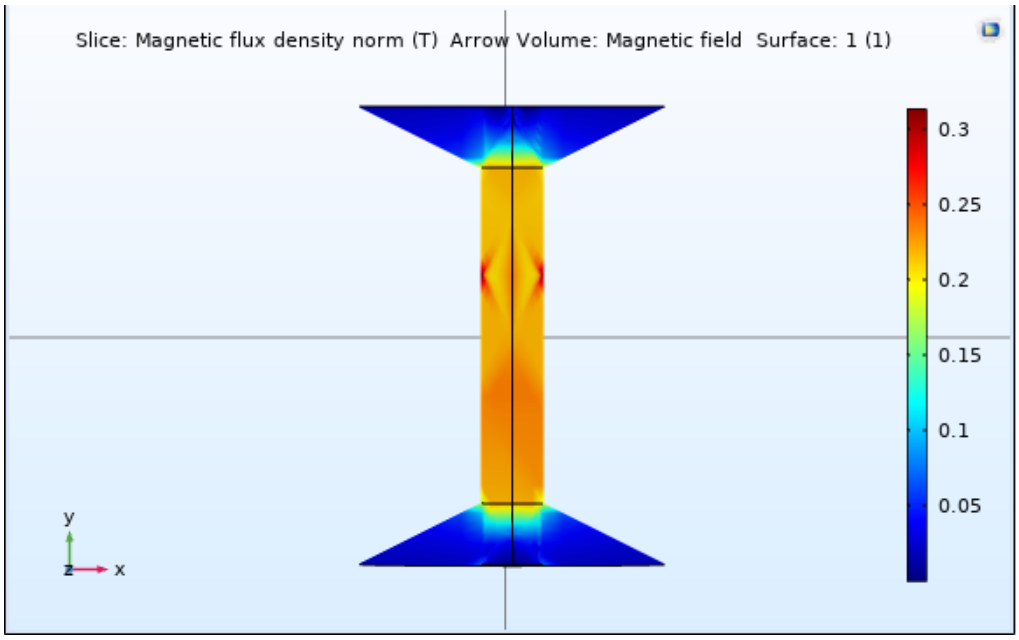

Figure 4.11: Bow-Tie model proposed by Yuan et al. [2] with uniform internal magnetic flux density of approximately 0.25T in the core

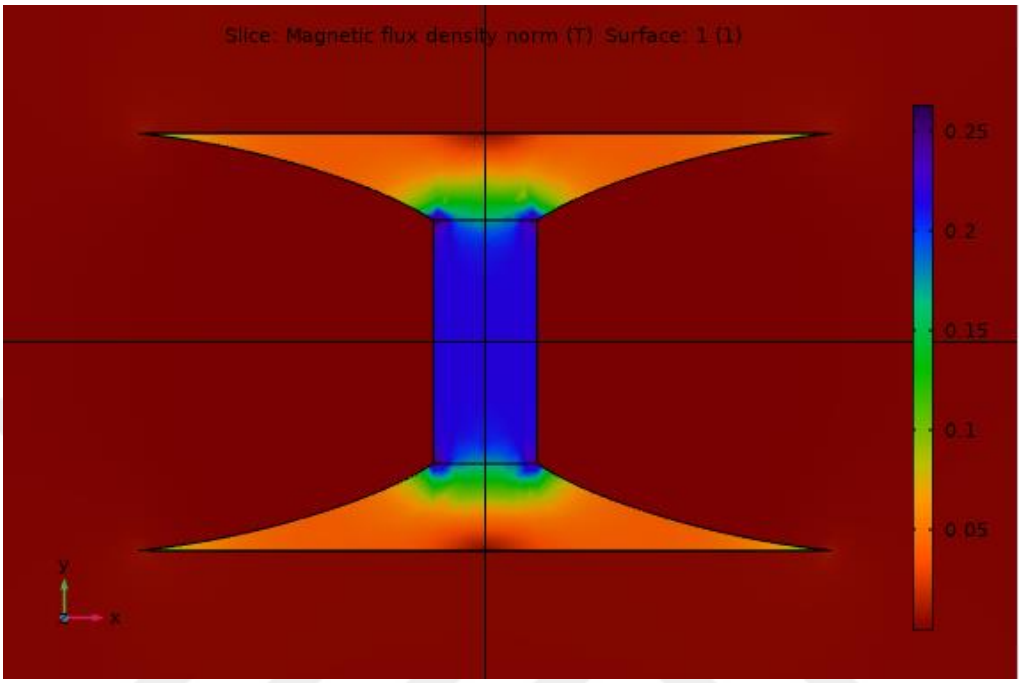

Figure 4.12: First attempt on Bow-Tie modification showing an average uniform magnetic flux density of 0.25T just like the original model.

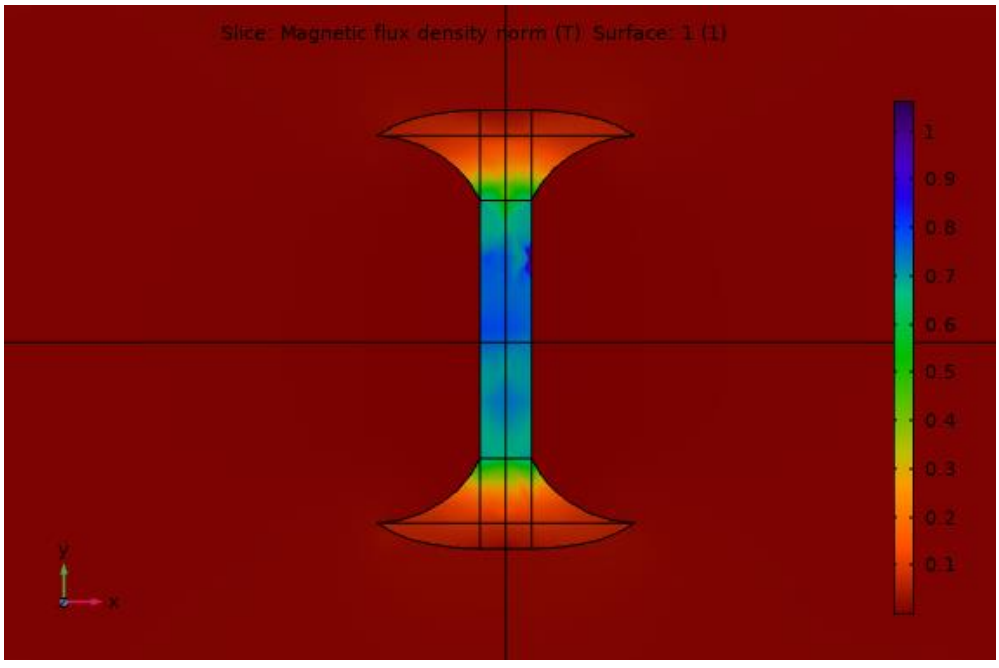

Figure 4.13: Final modification we call the Mushroom Head Core. This is the result of uniform magnetic flux density, which is almost 1T.

From the obtained result, I computed the current generated in the core using AWG 26 copper wire for winding and taking into account, weight [35]. From the dimension of my core geometry and provided material density, I got the overall weight of $1.65kg$ for our Silicon core Iron alloy. Therefore, using AWG 26 dimensions for 1000 turns of winding, I achieved an overall approximate core and coil assembly of about $1.75kg$. Using all the above stated condition – core size, wire gauge, number of turns, flux density, permeability etc., I calculated an induced current of 0.5mA at the output of the model.

5. CONCLUSION

5.1 CONCLUSION

These results and analysis demonstrate that sufficient power can be used wirelessly and simultaneously to charge hovering UAVs without unnecessary downtime. The values of the power generated will ensure a fast charging time. Because, considering the obtained result and the given approximate field space, the approximate flux density range can be calculated with a known required power to charge the drone. With an output current of 0.5mA, it will be easier to multiply the output voltage using an n-stage Crowcroft voltage doubler (to a voltage of, say 12V). Then, using current doubler, the voltage drops to half its value (6V) so as to increase the overall output current to 1A.

Now, considering a practical domestic drone battery parameter of 3.7V and 720mAH, which normally comes with a 5V / 1.2A charging adaptor, the power generated by the proposed model will comfortably charge such a drone. With this calculation it is safe to say that the drone can fly comfortably at a distance of about 10 meters away from the lines to charge, and at a higher altitude – in reference to the transmission tower – it can fly further away from the lines and still be within charging range.

Therefore, this research, which is a modification to the work from Yuan et al [2], has presented a practical WPT solution that can be implemented on a UAV. However, it can be optimized even further.

The induction coil's core material will increase the overall weight of the drone unit, which will make it consume more power and reduce its efficiency. Alloy cores of high relative permeability are expensive and not readily available at this time. For future research, lightweight materials that attract a strong flux field and are easily obtained should be considered.

Regarding cost-savings for power transmission, the billing cost of this project is not discussed in this paper.

Additionally, the use of Omni directional antennas would provide 360 degree coverage of RF frequency seeking, but the Omni directional antennas have a low gain factor. Hence, this work

have made use of directional antennas. To focus the antennas' array in the direction of a strong transmission frequency, a good positioning and signal scanning algorithm must be developed to achieve higher efficiency in practical applications.

5.2 FUTURE WORK

This thesis discusses the direct charging of drones from WPT energy sources. However, in the case of a drone fleet consisting of different types and functions, the proposed improvement to this work will be the design of a WPT harvesting power station, to serve as hub to accumulate and store electricity. The power station will incorporate wireless coupling charging pods or a platform for quick charging. This is an effort to move the substantial weight of charging components from UAVs to the charging pods.

REFERENCES

[1] N. M. Roscoe and M. D. Judd, “Harvesting energy from magnetic fields to power condition monitoring sensors,” *IEEE Sens. J.*, vol. 13, no. 6, pp. 2263–2270, 2013.

[2] S. Yuan, Y. Huang, J. Zhou, Q. Xu, C. Song, and P. Thompson, “Magnetic Field Energy Harvesting under Overhead Power Lines,” *IEEE Trans. Power Electron.*, vol. 30, no. 11, pp. 6191–6202, 2015.

[3] S. Levine and K. Kendall, “Energy Efficiency and Conservation : Opportunities , Obstacles , and Experiences,” *Vermont J. Environ. Lae*, vol. 8, no. 1, pp. 101–113, 2006.

[4] N. Tesla, “Apparatus for Transmitting Electrical Energy,” p. 4, 1914.

[5] M. Simic, C. Bil, and V. Vojisavljevic, “Investigation in wireless power transmission for UAV charging,” *Procedia Comput. Sci.*, vol. 60, no. 1, pp. 1846–1855, 2015.

[6] N. Bhushan *et al.*, “Network Densification: The Dominant Theme for Wireless Evolution into 5G,” *IEEE Commun. Mag.*, vol. 0163–6804, no. 14, pp. 82–89, 2014.

[7] A. Cimmino *et al.*, “The Role of Small Cell Technology in Future Smart City Applications,” *Trans. Emerg. Telecommun. Technol.*, vol. 2, no. 10, pp. 1–10, 2013.

[8] L. G. Tran, H. K. Cha, and W. T. Park, “RF power harvesting: a review on designing methodologies and applications,” *Micro Nano Syst. Lett.*, vol. 5, no. 1, 2017.

[9] L. Xie, Y. Shi, Y. T. Hou, W. Lou, H. D. Sherali, and S. F. Midkiff, “Bundling mobile base station and wireless energy transfer: Modeling and optimization,” in *Proceedings - IEEE INFOCOM*, 2013, pp. 1636–1644.

[10] O. Galinina, H. Tabassum, K. Mikhaylov, S. Andreev, E. Hossain, and Y. Koucheryavy, “On feasibility of 5G-grade dedicated RF charging technology for wireless-powered wearables,” *IEEE Wirel. Commun.*, vol. 23, no. 2, pp. 28–37, 2016.

[11] B. J. DeLong, A. Kiourti, and J. L. Volakis, “A Radiating Near-Field Patch Rectenna for Wireless Power Transfer to Medical Implants at 2.4 GHz,” *IEEE J. Electromagn. RF Microwaves Med. Biol.*, vol. 2, no. 1, pp. 64–69, 2018.

[12] R. Shadid and S. Noghanian, “A Literature Survey on Wireless Power Transfer for Biomedical Devices,” *Int. J. Antennas Propag.*, vol. 2018, p. 11, 2018.

[13] L. Hardell, M. Carlberg, and L. K. Hedendahl, “Radiofrequency radiation from nearby base stations gives high levels in an apartment in Stockholm, Sweden: A case report,” *Oncol. Lett.*, vol. 15, no. 5, pp. 7871–7883, 2018.

[14] M. Moradi, N. Naghdi, H. Hemmati, M. Asadi-Samani, and M. Bahmani, “Effect of Ultra High Frequency Mobile Phone Radiation on Human Health,” *Electron. Physician*, vol. 8, no. 5, pp. 2452–2457, 2016.

[15] A. Kurs, “Power Transfer Through Strongly Coupled Resonances,” 2007.

[16] A. Kurs, A. Karalis, R. Moffatt, and J. D. Joannopoulos, “Wireless Power Transfer via Strongly Coupled Magnetic Resonances,” *Science (80-.).*, vol. 317, no. 5834, pp. 83–86, 2007.

[17] M. Lu, M. Bagheri, A. P. James, and T. Phung, “Wireless Charging Techniques for UAVs: A Review, Reconceptualization, and Extension,” *IEEE Access*, vol. 6, pp. 29865–29884, 2018.

[18] X. Mou and H. Sun, “Wireless power transfer: Survey and roadmap,” *IEEE Veh. Technol. Conf.*, vol. 2015, no. 646470, pp. 1–13, 2015.

[19] K. Paul and A. K. Sarma, “Fast and efficient wireless power transfer via transitionless quantum driving,” *Sci. Rep.*, vol. 8, no. 1, pp. 1–10, 2018.

[20] MIT, “Faraday’ s Law of Induction,” *Science*, 2009. [Online]. Available: http://web.mit.edu/8.02t/www/802TEAL3D/visualizations/coursenotes/modules/guide10.pdf.

[21] J. Caxias, F. A. Silva, and J. Sequeira, “Transmission line inspection robots: Design of the power supply system,” *2010 1st Int. Conf. Appl. Robot. Power Ind. CARPI 2010*, pp. 1–6, 2010.

[22] R. M. White, D. S. Nguyen, Z. Wu, and P. K. Wright, “Atmospheric sensors and energy

harvesters on overhead power lines," *Sensors (Switzerland)*, vol. 18, no. 1, 2018.

[23] V. Gupta, A. Kandhalu, and R. (Raj) Rajkumar, "Energy harvesting from electromagnetic energy radiating from AC power lines," p. 1, 2011.

[24] R. Horton, M. Halpin, and K. Wallace, "Induced voltage in parallel transmission lines caused by electric field induction," *Proc. IEEE Int. Conf. Transm. Distrib. Constr. Live Line Maintenance, ESMO*, pp. 1–7, 2006.

[25] Y. Luo *et al.*, "Analysis of Induced Voltage of Parallel UHV Double-circuit AC Transmission Lines," *IOP Conf. Ser. Mater. Sci. Eng.*, vol. 452, no. 3, 2018.

[26] W. Pan, S. Miu, G. Yu, T. Wu, and B. Zhang, "Measurement and Simulation of Induced Voltage and Current on 110 KV Crossing Transmission Lines under UHV AC Transmission Lines," *Energy Power Eng.*, vol. 09, no. 04, pp. 635–643, 2017.

[27] M. Simic, C. Bil, and V. Vojisavljevic, "Investigation in wireless power transmission for UAV charging," *Procedia - Procedia Comput. Sci.*, vol. 60, pp. 1846–1855, 2015.

[28] M. N. . P. Kumar, K. A. Kumar, and D. C. Srinivasu, "Performance Analysis of Rectenna Using Closed Form Equation," *IOSR J. Electron. Commun. Eng.*, vol. 9, no. 4, pp. 37–41, 2014.

[29] J. Zhang, "RECTENNAS FOR RF WIRELESS ENERGY HARVESTING," University of Liverpool, 2013.

[30] S. Y. Liao, "Measurements and Computations of Electric Field Intensity and Power Density," *IEEE Trans. Instrum. Meas.*, vol. 26, no. 1, pp. 53–57, 1977.

[31] L. L. Grigsby and M. Reta-Hernández, "Transmission Line Parameters," in *Electric Power Generation, Transmission, and Distribution: The Electric Power Engineering Handbook*, 2019, pp. 14-1-14–36.

[32] M. Palati *et al.*, "Induced Voltage in Parallel Transmission Lines Caused by Electric Field Induction," *Energy Power Eng.*, vol. 9, no. 1, pp. 1–7, 2017.

[33] A. Hilal and B. Cougo, "Optimal inductor design and material selection for high power

density inverters used in aircraft applications," *2016 Int. Conf. Electr. Syst. Aircraft, Railw. Sh. Propuls. Road Veh. Int. Transp. Electrif. Conf. ESARS-ITEC 2016*, 2017.

[34] C. McLyman, *Transformer and Inductor Design Handbook, Fourth Edition*, Fourth. California: Marcel Dekker, Inc, 2011.

[35] R. (Ness E. I. . Ness, "Bare Copper Wire Data," *Ness Engineering Inc.*, 2017. [Online]. Available: http://www.nessengr.com/technical-data/bare-copper-wire/.

APPENDIX A

A.1 INDUCTANCE RELATIONSHIP WITH INDUCTION VOLTAGE

$$L = \frac{\mu_0 A N^2}{i}$$

$$L = \frac{N\Phi}{i}$$

$$A = \frac{1}{4.44 f B_m T_e}$$

Current Density

$$\delta = \frac{I}{A_{wire}}$$

$$N = T_e V$$